JOURNAL OF Applied Polymer SCIENCE

Properties of Polyimide Hybrids with Mixed Metal Oxide

Hsu-Tung Lu, Shih-Liang Huang, I-Hsiang Tseng, Yin-Kai Lin, Mei-Hui Tsai
Department of Chemical and Materials Engineering, National Chin-Yi University of Technology, Taichung 411, Taiwan, Republic of China

Correspondence to: M.-H. Tsai (E-mail: tsaimh@ ncut.edu.tw)

ABSTRACT: Polyimide/silica–titania (PI/SiO_2–TiO_2) hybrid films were prepared via an *in situ* sol–gel process. The PI precursor, poly(amic acid) (PAA), which contains 2,2'-bis[4-(4-aminophenoxy)-phenyl]propane (p-BAPPP), 3,3',4,4'- benzophenetetracarboxylic anhydride (BTDA) and 3-aminopropyltrimethoxysilane (APrTMOS), was first synthesized; this was followed by the addition of phenyltrimethoxysilane (PTMS) and/or tetraethyl orthotitanate ($Ti(OEt)_4$) to fabricate PI/SiO_2–TiO_2 films. The relative content of SiO_2 to TiO_2 has remarkable effects on the crosslink structure and resultant properties of the hybrids. XPS results confirm that the amount of Si on the surface of the hybrids is higher than that in the bulk. The distribution of Ti in the hybrid films is contrary to the above trend because of the formation of three-dimensional Si—O—Si, Si—O—Ti, and Ti—O—Ti networks. The SiO_2 content of the hybrids containing only silica significantly affects their refractive index, contact angle, and dielectric constant. The films with added PTMS show higher contact angles than pure PI because nonpolar segments, —C_2H_6 or benzene groups, tend to distribute on the surface. Upon the addition of ($Ti(OEt)_4$), some hydrophilic segments on the surface of the hybrids are induced because of the formation of a crosslinked structure. The denser crosslinked molecular structure, and consequently lower CTE and higher T_g are obtained from hybrids containing more TiO_2. By comparing the above properties and flexibility, the best composition of metal oxides (SiO_2/TiO_2) in hybrids is 20/80. That is, an optimum ratio of metal oxides in PI hybrids induces superior properties for advanced practical applications. © 2012 Wiley Periodicals, Inc. J. Appl. Polym. Sci. 000: 000–000, 2012

KEYWORDS: polyimide; sol–gel; hybrid; mixed metal oxide; thermal properties; refractive index

Received 24 May 2011; accepted 2 April 2012; published online
DOI: 10.1002/app.37865

INTRODUCTION

Organic/inorganic hybrid films have become an effective source of advanced materials as they exhibit excellent properties that other composites and conventional materials do not possess.[1,2] Those hybrids combine the beneficial properties of inorganic materials with rigidity, high thermal stability, and mechanical strength as well as the organic polymers with flexibility, ductility, and easy processability.[3–5] Through sol–gel process, there are many successfully prepared polyimide (PI)/inorganic materials hybrid thin films with a wide range of material properties, such as high thermal stability, high mechanical strength, flexibility, and easy processability.[6–15] Certain properties, such as high glass transition temperature (T_g), low CTE and low dielectric constant, and hydrophobicity, are desirable for materials in modern electrical usages. An enhanced thermal conductivity of PI was also achieved by incorporation of SiO_2 or TiO_2 in PI matrix.[13] Recently, researchers also reported the improved properties of PI films with the combination of two or more inorganic metal oxides.[16–20] The introduction of TiO_2 and SiO_2 in PI matrix will increase the refractive index and the thermal stability, respectively.[16] The presence of SiO_2 in PI/SiO_2–TiO_2 hybrid films restricts the aggregation of TiO_2 particles and remains the transparency of hybrid films when the total inorganic content is less than 5 wt %.[17] The addition of inorganics in PI matrix always sacrifices the optical transparency. Another literature[18] reported that PI/SiO_2–TiO_2 hybrid composite remains excellent optical transmittance at 500 nm (>90%) when the SiO_2 content of is 15 wt % and TiO_2 is less than 5 wt %.

The optical transparency, film processability, flexibility, and contact angle of PI hybrids with high TiO_2 content are inferior to those of PI hybrid with SiO_2. However, other properties, such as T_g and CTE, are generally superior in PI hybrids containing TiO_2. Hence, a combination of the superiority of two types of metal oxides in PI films is sought to expand the respective characteristics of inorganics and obtain better properties of PI hybrids.[14,15,18] While, the reactivity of alkane metal oxides is

different and ranking in the following sequence: $Zr(OR)_4$, $Al(OR)_3$ > $Ti(OR)_4$ > $Sn(OR)_4$ >> $Si(OR)_4$. Moreover, the surface energy is different, $TiO_2 > Al_2O_3 > SiO_2$, that silica can easily be dispersed on the surface of PI film and titania tends to be in the bulk. When adding more than one metal oxide into PI matrix, the abovementioned two phenomena will affect the distribution of metal oxides and the crosslink structures, Si—O—Si, Ti—O—Ti, and Si—O—Ti, in the PI matrix. Consequently, the silica/titania ratio in PI matrix can be adjusted to get distinct properties for a wide range of applications, such as optical device or flexible printed circuit.

The goal of this manuscript is to synthesize PI hybrids containing mixed metal oxides, silica, and titania, and also to investigate the effects of mixed oxides on the thermal properties, flexibility, refractive index, and hydrophobicity of resultant hybrids. In this study, APrTMOS was used as a coupling agent to control the chain length of PI segment of 10,000 g/mole. The practically favorable monomers BTDA and BAPP were selected to systematically synthesize PI hybrid films containing various amounts of SiO_2 and TiO_2. The compromised ratio of SiO_2/TiO_2 in PI matrix was sought to get a PI hybrid for the applications in the optical or electrical industry.

MATERIALS AND METHODS

Materials

3,3',4,4'-Benzophenetetracarboxylic anhydride (BTDA, courtesy from Taimide Tech. Inc.) was purified by recrystallization from acetic anhydride and then dried in a vacuum oven at 120°C overnight. 2,2'-Bis[4-(4-aminophenoxy)phenyl] propane (p-BAPP, courtesy from Taimide Tech. Inc.) was dried in a vacuum oven at 125°C for 24 h prior to use. 3-Aminopropyltrimethoxysilane (APrTMOS) was obtained from Tokyo Chemical Industry. *N, N*-Dimethylformamide (DMF, 99.5%) from Fisher Chemical Company was dehydrated with 4 Å molecular sieves. Tetraethyl orthotitanate ($Ti(OEt)_4$) and acetylacetone (ACAC) from Tokyo Chemical Industry and phenyltrimethoxysilane (PTMS, $PhSi(OCH_3)_3$ or PhSiOx, 97%) from Alfa Aesar were used as supplied.

Synthesis of PI/SiO_2–TiO_2 Hybrid Films

The synthesis process of PI/SiO_2–TiO_2 hybrid films is presented in Scheme 1. In a three-necked flask, p-BAPP and DMF were mixed with a mechanical stirrer for about 10 min under nitrogen to thoroughly dissolve p-BAPP in DMF. Equal molar BTDA was added in five sequences and completely dissolved in the diamine solution. APrTMOS with monoamine group was added to the above solution and stirred for 1 h to control the PI segment with the chain length of 10,000 g/mole.[7,8] The poly (amic acid) (PAA) solution with the solids content of 18 wt % was then obtained. Various amounts of PhSiOx, $Ti(OEt)_4$, and ACAC (molar ratio of $Ti(OEt)_4$ to ACAC = 1/4.1) were completely mixed with PAA solution for at least 12 h to obtain the modified PAA solution. The PI precursor was coated on PET films or glass substrates using a doctor-blade. The coated films were then cured in an oven at a heating rate of 1.5°C/min from 80 to 170°C (thermal set for 90 min) and to 300°C (thermal set for 30 min). After the curing process, the hybrid films were peeled from glass substrates after immersion in water bath. The thickness of pure PI, PIS, and PIS hybrid films is in the range of 25–30 μm.

The sample code is presented by PIS-X-SYTZ, where PIS indicates APrTMOS-containing PI films with a chain length of 10,000 g/mole. *X* is the total inorganic content (wt %) in hybrids based on the assumptions of complete imidization, complete conversion of $Ti(OEt)_4$ to titania and no residual solvent. *Y* and *Z* represent the relative weight ratio of PhSiOx to TiO_2. A reference sample, pure PI, contains only p-BAPP and BTDA. In this study, the discussion is focused on PIS samples with total inorganic content of 8 wt %. The relative molar ratio of PhSiOx to TiO_2 is 10/0 (only PhSiOx), 8/2, 5/5, 2/8, and 0/10 (only TiO_2). For example, PIS-8%-S2T8 is the PIS hybrid with 8 wt % of metal oxides containing 20 wt % PhSiOx and 80 wt % TiO_2. As the total metal oxide content exceeds 8 wt %, the hybrids were brittle. That is, 8 wt % of PhSiOx and TiO_2 may be the largest added amount in this PI system. The monomer composition of pure PI and hybrids is summarized in Table I.

Measurements

X-ray photoelectron spectroscopic (XPS) spectra were obtained by using an ESCA ULVAC-PHI spectrometer working in the constant analyzer energy mode with a pass energy of 50 eV and the excitation source of Al Kα (280 eV) radiation. XPS analysis was done at room temperature and at the pressure below 5×10^{-10} Torr. The take-off angle used in the XPS depth-profiling was 45° and the sputtering rate was 10 nm/min. The Fourier transform infrared (FTIR) spectra of pure PI and PIS hybrid films were recorded by a Nicolet Protégé-460 FTIR spectrophotometer (FTIR). The UV–vis spectra of PIS hybrid films were performed with a Shimadzu UV1800 spectrophotometer. The color intensity of polymers was determined by a color meter (X-Rite SP60, USA). Measurements were performed with films, using an observational angle 10° and a CIE (Commission Internationale de ÍEclairage)-D65 illuminant. A CIE color different equation based on ASTM E313-98 was used to evaluate the L^*, a^*, b^* values. The contact angle of water droplets on hybrid films was measured using a goniometer (DSA10-MK2) equipped with a camera to capture images of water droplets at room temperature on the surface of hybrid films. The contact angle of each film presented in this study was an average of the contact angles from five droplets at different locations of each film. The sample was spin-coated on a silicon wafer for refractive index measurement. The in-plane and out-of-plane refractive indices (n_{TE} and n_{TM}, respectively) at room temperature were measured using a prism coupler (Metricon, 2010) at the wavelength of 1310 nm. The dielectric constant (k) was calculated from the following formula $k = Cd/A\varepsilon_o$, where C is the observed capacitance, d is the film thickness, A is the area of gold, and ε_o is the free permittivity based on the standards of ASTM D-150-95 and IPC-TM-650, m2.5.5.3.

The dynamic mechanical analysis (DMA) was performed on a thermal analyzer (DMA-2980, TA Instruments) at a heating rate of 3°C/min, from 60 to 450°C, and at the frequency of 1Hz. Thermogravimetric analysis (TGA) was carried out with a thermal analyzer (TGA-2050, TA instruments) at a heating rate of 20°C/min, from 50 to 700°C, and under air atmosphere. The polymer decomposition temperature (Td) was determined at the weight loss of 5 or 10%. The coefficient of thermal expansion (CTE) was characterized using a thermal mechanical analyzer (TMA-2940, TA instruments) with a fixed tension force of

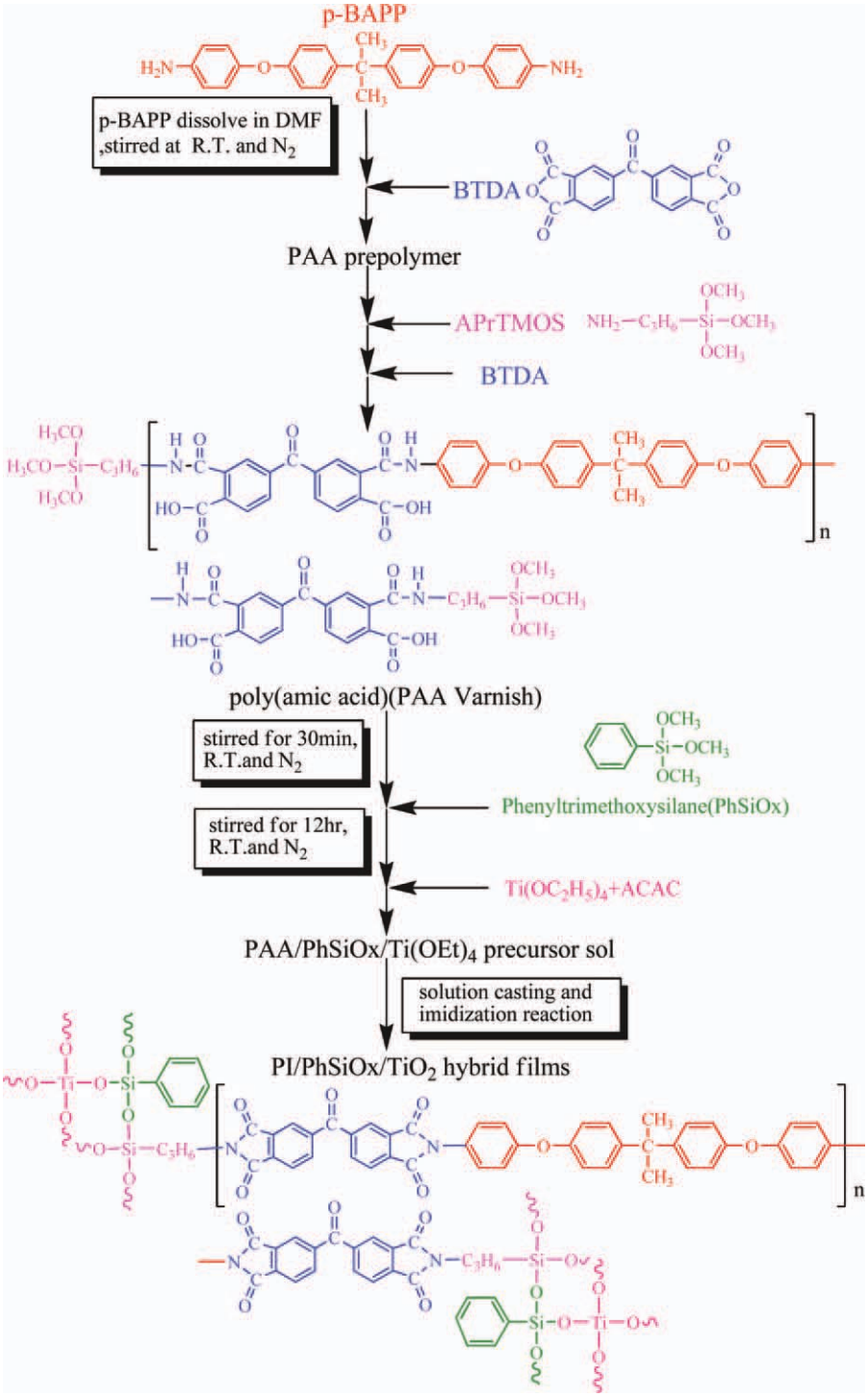

Scheme 1. Synthesis process of PI/PhSiOx/TiO_2 hybrid films. [Color figure can be viewed in the online issue, which is available at wileyonlinelibrary.com.]

0.05 N, in the temperature range of 50 to 350°C and at a heating rate of 10°C/min. The CTE values were determined as the dimension changes within the temperature range of 100–200°C. The measurement of dielectric constant (k) of each sample was performed on an impedance analyzer (Agilent 4294A) at the frequency of 1–100 MHz. Both surfaces of film samples were coated with gold before measurement.

RESULTS AND DISCUSSION

Distribution of Metal Oxides in PIS Hybrid Films

The XPS results of PhSiOx or TiO_2 presented in PI hybrid films were shown in Figures 1–5. No characteristic Si or Ti peaks were observed for pure PI. As shown in Figure 1, the characteristic Si_{2p} and Si_{2s} peaks were presented in XPS survey spectra of PIS and PIS-8%-S2T8 films owing to the addition of

Table I. Weight Composition of Pure PI, PIS, and PI/PhSiOx-TiO_2 Hybrid Films

	Weight composition (g)				
Sample	BTDA	p-BAPP	APr TMOS	PhSiOx	$Ti(OEt)_4$
Pure PI	4.418	5.222	0	0	0
PIS	4.418	5.222	0.36	0	0
PIS-8%-S10T0	4.418	5.222	0.36	0.80	0
PIS-8%-S8T2	4.418	5.222	0.36	0.64	0.16
PIS-8%-S5T5	4.418	5.222	0.36	0.40	0.40
PIS-8%-S2T8	4.418	5.222	0.36	0.16	0.64
PIS-8%-S0T10	4.418	5.222	0.36	0	0.80

APrTMOS, which contains Si element. In addition to the Si_{2p} and Si_{2s} peaks, the Ti_{2p} characteristic peaks were visible in PIS-8%-SYTZ films ($Z \neq 0$). Other XPS spectra, C_{1s} and N_{1s}, were clearly presented on all samples with positions consistent to the literature. Figure 2 depicts the O_{1s} spectra of PIS-8%-S2T8 film. Three characteristic O_{1s} peaks of Si—O—Si,[19] Ti—O—Ti, and Si—O—Ti[20,21] were derived from Guassian deconvolution fitting procedure. The presence of these characteristic peaks indicated the formation of crosslinked structures between PhSiOx and $Ti(OEt)_4$ in the PI matrix through sol–gel process.

Figures 3 and 4 present the binding energies of $Ti_{2p3/2}$, $Ti_{2p1/2}$, and Si_{2p} photoelectrons peaks of PIS-8%-S2T8 films under various sputtering times during XPS measurement. There are two Ti_{2p} binding energy peaks as a result of Ti atom in the different chemical environments. The characteristic Ti_{2p} photoelectrons peaks at 456.2 and 462.2 eV[22–24] were observed within the films. The binding energy of Ti at the surface (sputtering time = 0 sec) of the hybrid film was higher than that in the bulk (sputtering time > 0 sec) of film. The reason is due to molecular oxygen in the air-side of films induced the transformation of $Ti(OEt)_4$ to TiO_2, whose Ti has higher binding energy. Different kinds of titanium compounds, such as Ti—C and Ti—O,[25,26]

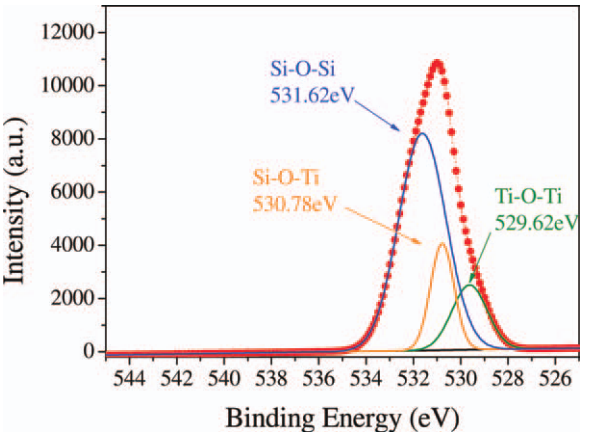

Figure 2. XPS (O_{1s}) spectrum of PIS-8%-S2T8 (solid dots) with Guassian deconvolution fitting results (lines). [Color figure can be viewed in the online issue, which is available at wileyonlinelibrary.com.]

might exist in the PIS hybrid films as well. While, the Si binding energy at 101.4 eV and 100 eV was observed for the surface and the bulk of the PIS-8%-S2T8, respectively.

The inorganic content of Si or Ti in the PIS-8%-S2T8 film was shown in Figure 5 as a function of sputtering time. Before sputtering, the relative atomic ratio of Si/Ti was around 55/45. The composition of Ti was increased with the sputtering time indicating more Ti distributing in the bulk than in the surface. In contrast, the Si concentration in the bulk was less than that on the surface. The surface content of Si was higher than that of Ti. There are two explanations for the above phenomena: First, the surface energy of Si (866 erg/cm^2, 25°C) is lower than that of Ti (1979 erg/cm^2, 25°C). Si can easily migrate to the surface and Ti tends to disperse in the bulk of film.[27] Second, the reactivity of $PhSiO_x$ to silica is lower than that of $Ti(OEt)_4$ to titania due to the steric hindrance of benzene group. The binding energy of Ti—O—Ti is larger than that of Si—O—Si group as well as the crosslinkage density of Ti—O—Ti is higher than that

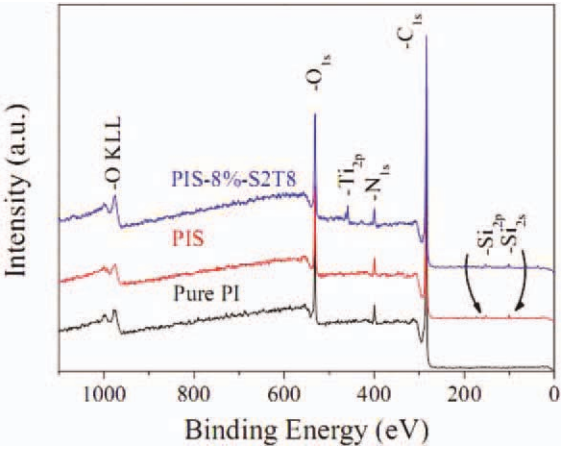

Figure 1. XPS survey spectra of pure PI, PIS, and PIS-8%-S2T8 films. [Color figure can be viewed in the online issue, which is available at wileyonlinelibrary.com.]

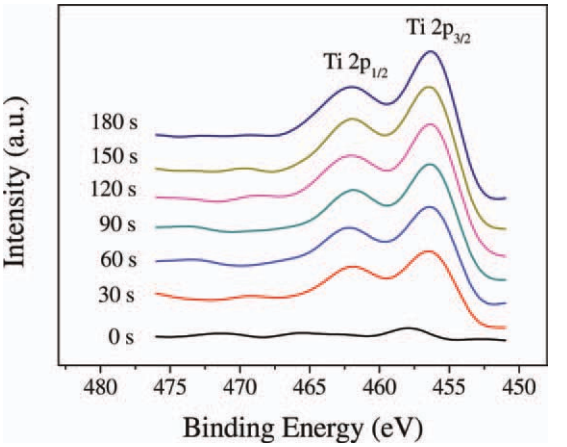

Figure 3. XPS (Ti_{2p}) spectra of PIS-8%-S2T8 hybrid film recorded at different sputtering time. [Color figure can be viewed in the online issue, which is available at wileyonlinelibrary.com.]

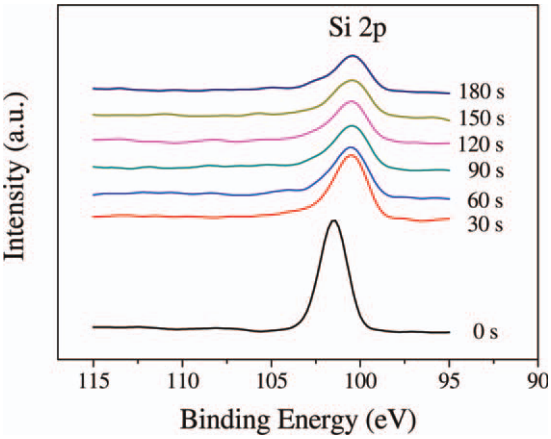

Figure 4. XPS (Si_{2p}) spectra of PIS-8%-S2T8 hybrid film recorded at different sputtering time. [Color figure can be viewed in the online issue, which is available at wileyonlinelibrary.com.]

of Si—O—Si group. Consequently, Ti element is more or less easily dispersed in the bulk of film.

The FTIR spectra shown in Figure 6 also confirmed the presence of characteristic peaks for Si—O—Si (1000–1100 cm^{-1}), Ti—O—Si (~940 cm^{-1}), and Ti—O—Ti (450–850 cm^{-1}) structures on PIS hybrid films.[18] Moreover, the characteristic imide absorption bands at 1380 cm^{-1} (C—N stretching), 1700 cm^{-1} and 1780 cm^{-1} (symmetrical and asymmetrical C=O stretching) were observed on the IR spectra of cured PIS hybrid films indicating the completely imidization in each film.

Thermal Properties of PIS Hybrid Films

The DMA results of pure PI and PIS hybrid films are shown in Figure 7 and Table II. The maximum of each tan δ curve was assigned as the T_g value of each film. The T_g value of pure PI (251.7°C) slightly increased to 255.6°C for PIS, and then decreased to 247.9°C for PIS-8%-S10T0. There were two contrary effects on T_g values. The T_g value increases as the crosslinkage formed through APrTMOS and PhSiOx. A more complete crosslinkage will be produced in PI matrix with the presence of APrTMOS rather than PhSiOx. The benzene rings

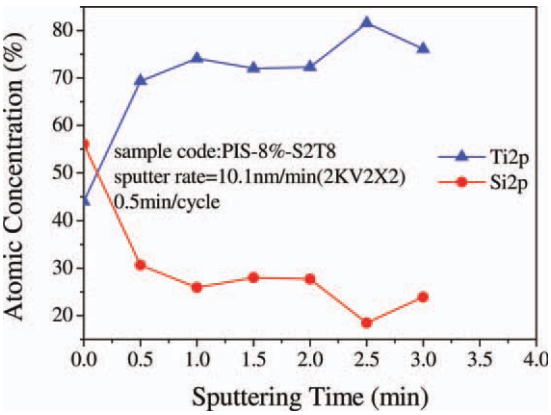

Figure 5. Effect of sputtering time on the Si or Ti atomic concentration of PIS-8%-S2T8 film. [Color figure can be viewed in the online issue, which is available at wileyonlinelibrary.com.]

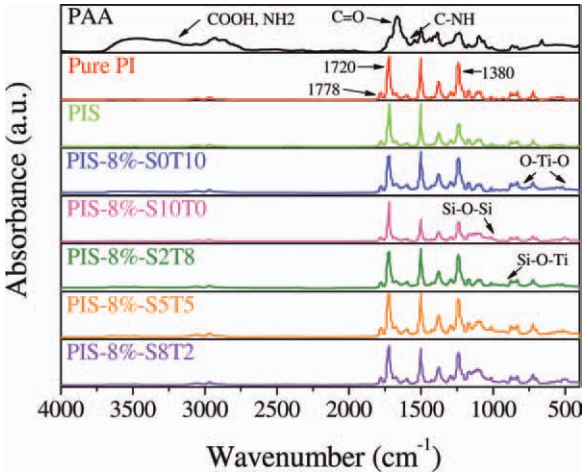

Figure 6. FTIR spectra of pure PI and PIS hybrid films. [Color figure can be viewed in the online issue, which is available at wileyonlinelibrary.com.]

of PhSiOx hinder the formation of crosslinkage and affect the intermolecular attraction. Consequently, the free volume of PI with the presence of PhSiOx will be enlarged that the T_g value decreases.

The increase in T_g value was observed for PIS hybrid films with the increasing TiO_2 contents. The T_g value of PIS-8%-series hybrids increased from 247.9°C for -S10T0 to 263.3, 283.2, 316.7, and 331.7°C for S8T2, S5T5, S2T8, and S0T10, respectively. A stronger and more complete crosslinkage was formed between the added $Ti(OEt)_4$ groups in the PI matrix that a higher T_g value was obtained.

The CTE values of pure PI, PIS, and hybrids determined from TMA results (Figure 8) in the temperature range of 100 to 200°C were listed Table II. The pure PI, PIS, and hybrids exhibit CTEs in the range of 58–68 ppm/°C. The addition of APrTMOS and inorganics slightly increased the CTE that the CTEs of PIS and its hybrids were higher than that of pure PI. The CTE of

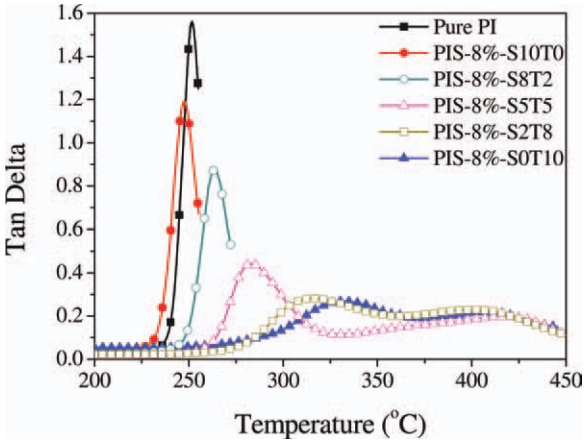

Figure 7. The tanδ curves of pure PI and PI/PhSiOx/TiO_2 hybrid films. [Color figure can be viewed in the online issue, which is available at wileyonlinelibrary.com.]

Table II. Thermal Properties of Pure PI, PIS, and PI/PhSiOx-TiO_2 Hybrid Films

	TGA		TMA	DMA
Sample	Td (5 wt %) (°C)	Td (10 wt %) (°C)	CTE (100–200°C) (ppm/°C)	T_g (°C)
Pure PI	518.5	531.7	58.4	251.7
PIS	513.5	527.3	64.2	255.6
PIS-8%-S10T0	528.5	541.3	67.7	247.9
PIS-8%-S8T2	506.5	531.2	67.5	263.3
PIS-8%-S5T5	484.1	517.5	62.8	283.2
PIS-8%-S2T8	470.2	516.1	59.5	316.7
PIS-8%-S0T10	473.1	515.4	58.6	331.7

PIS-8%-S10T0 is 67.7 ppm/°C compared with 64.2 ppm/°C for PIS and 58.4 ppm/°C for pure PI. For PIS-8%-hybrids containing TiO_2, the CTE value decreased with the increasing TiO_2 content. The intermolecular cross-linkage will decrease the CTEs of hybrids, while the steric hindrance of benzene ring will enlarge the free volume and then increase the CTEs. The benzene rings and three —OCH_3 groups in PhSiOx lead to the formation of loosely cross-linked structure due to the steric hindrance of benzene ring and low reactivity of —$Si(OCH_3)_3$ groups. The competition of the above two contrary effects is responsible for the changes in CTEs of hybrid films.

The thermal stability of pure PI and other hybrid films with different inorganic contents were examined by TGA and the results are shown in Table II and Figure 9. The hybrid films began to decompose around 400°C. The decomposition temperature at 5% weight loss (Td, 5 wt %) was ranging from 470.2 and 528.5°C. The effect of oxide composition on the changes of Td (5 wt %) was similar to that of Td (10 wt %). A slight decrease in Td (10 wt %), from 531.7°C to 527.3°C, was observed when the pure PI was incorporated with APrTMOS, i.e., pure PIS. When adding 8% of silica within PIS matrix, the Td (10 wt %) of PIS-8%-S10T0 increases significantly to 541.3°C. However,

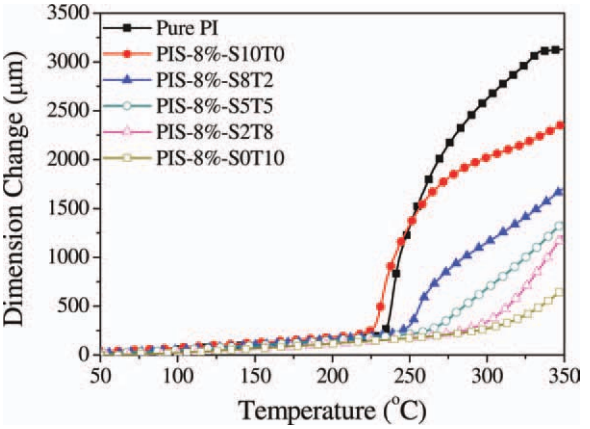

Figure 8. The dimension change of pure PI and PI/PhSiOx-TiO_2 hybrid films as a function of temperature. [Color figure can be viewed in the online issue, which is available at wileyonlinelibrary.com.]

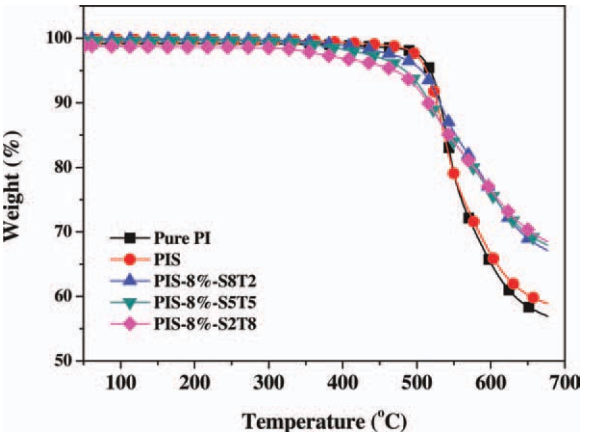

Figure 9. TGA curves of pure PI, PIS and PIS hybrid films. [Color figure can be viewed in the online issue, which is available at wileyonlinelibrary.com.]

further decrease in thermal stability was observed when SiO_2 was substituted by TiO_2. The Td (10 wt %) of PIS-8%-S0T10 hybrid, which contains 8 wt % TiO_2, was 515.4°C. The presence of TiO_2 compounds could cause a catalytic degradation of polyimide films.[18,28–30]

The changes in Td (5 or 10 wt %) are also corresponding to the PI surface containing more nonpolar soft segment but less hard segment, such as benzene or Si—O—Si. The addition of APrTMOS and PhSiOx increases the cross-linkage and then parts of nonpolar soft segments, such as -C_3H_6 and -CH_3, are pushed to the film's surface resulting a decrease in Td. Meanwhile, a crosslinkage structure dispersed on film's surface will enhance the intermolecular structure and then increase the Td value. The nonpolar soft segment on film's surface may possess superior effect on the Td value that the Td values decreased at the initial stage of introduction of APrTMOS. In contrast, the Td value increases with PhSiOx presenting in PI, where the crosslinked component may possess superior effect on the Td value. The decrease in Td values of PIS hybrids with increasing Ti content may also be the result of the stronger cross-linkage and more nonpolar soft segments presenting on the surface.

Mechanical Properties of PIS Hybrid Films

Figure 10 shows the storage modulus of pure PI and PIS hybrid films as the function of temperature. At low temperature (60°C), the storage modulus of PIS hybrid films is higher than that of pure PI (2040 MPa). When adding 8% of silica within PIS matrix, the storage modulus of PIS-8%-S10T0 increases significantly to 3189 MPa. Substituting 20 wt % SiO_2 with TiO_2 reduces the storage modulus to 2178 MPa for PIS-8%-S8T2. Further increasing in TiO_2 content increases the storage modulus, which reaches 3630 MPa for PIS-8%-S2T8 film. In contrast, the storage modulus of PIS-8%-S0T10, containing 8% of TiO_2, is slightly lower than that of PIS-8%-S10T0. The storage modulus is enhanced by substituting SiO_2 with TiO_2 until PIS hybrids containing equal amount of two oxides. On the other hand, the increase in storage modulus at high temperature (> 300°C) was observed for PIS hybrid films with increasing TiO_2. The presence of TiO_2 in PI leads to the formation of cross-linkage

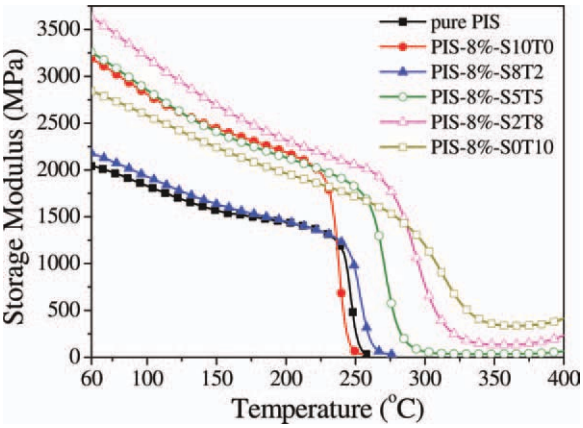

Figure 10. The storage modulus of pure PI and PI/PhSiOx-TiO_2 hybrid films as a function of temperature. [Color figure can be viewed in the online issue, which is available at wileyonlinelibrary.com.]

structure that PIS hybrids retain excellent mechanical strength even at high temperature.

Dielectric Constant

The dielectric constants of pure PI and PIS hybrid films are depicted in Table III. The addition of PhSiOx leads to the decrease in dielectric constant. The dielectric constant of pure PI is 3.33 and decreases to 3.27 and 3.26 for pure PIS and PIS-8%-S10T0, respectively, with more Si (including PhSiOx and APrTMOS) presenting in films. The addition of APrTMOS and PhSiOx, which contains nonpolar segments -C_3H_6 and benzene group, increases the nonpolarity of the films and then decreases the dielectric constant. Besides, the reaction of $PhSi(OCH_3)_3$ may not complete that some of the nonpolar -CH_3 segments remain in the films. There are Si—O—Si polar segments presenting in hybrids, however, the above mentioned nonpolar segments show superior effects on the changes in dielectric constants.

On the other hand, the increase in dielectric constant was observed when the Ti content in PIS hybrids increases. The dielectric constant is 3.26 for hybrids without TiO_2, PIS-8%-S10T0, and increased to 3.46, 3.52, 3.69, and 3.87 for PIS hybrids containing 1.6, 4.0, 6.4 to 8 wt % Ti, respectively. One reason is because of the higher dielectric index of TiO_2. However, the increase in dielectric constant that of hybrids with mixed metal oxides is not significant due to the contrary effect of PhSiOx and TiO_2 on the dielectric content. The PhSiOx containing benzene ring and three —OCH_3 groups provides the steric barrier that the reactivity is relatively low. Both the randomly formed crosslinked structure and the steric hindrance will decrease the value of dielectric content. Besides, the reactivity of metalkoxides is decreased in the following sequence: $Zr(OR)_4$, $Al(OR)_4$ > $Ti(OR)_4$ > $Sn(OR)_4$ >> $Si(OR)_4$. The reactivity of $Ti(OEt)_4$ is higher than $PhSi(OCH_3)_3$ groups. The Ti—O—Ti crosslinked structures are easily formed with more ordered arrangement and more polar segments are induced. Consequently, a little increase in dielectric constant of hybrids with the addition of $Ti(OEt)_4$ is revealed.

Contact Angle

Contact angle analysis provides the information of hydrophobicity at the air–water–solid interface. Surface with large contact angles means very hydrophobic surface, such as silicon or fluorocarbon polymers. A highly hydrophilic surface, such as glass or mica, will present low contact angle. The results of contact angles (or surface energies) of pure PI and hybrids are demonstrated in Table III. The contact angle is 60.8° for pure PI and increases to 78.8° and 85.7° for pure PIS and PIS-8%S10T0, respectively. More Si components are dispersed on the film surface upon the addition of APrTMOS and PhSiOx, which contain hydrophobic components. The increase in intermolecular cross-linkage will push more nonpolar segments, such as -C_2H_6 or benzene groups, migrating to the surface, while the polar segments, such as Si—O—Si or Ti—O—Ti segments, will remain within the bulk of the film. The contact angle of films is thus increased in the following rank: pure PI < pure PIS < PIS-8%-S10T0.

On the other hand, the contact angle of titania-containing hybrids is smaller than that of only silicon-containing hybrids. The contact angle is 85.7°for PIS-8%-S10T0 and decreases to 82.1°, 81.2°, 74.5°, and 74.2° for PIS-8%-S8T2, -S5T5, -S2T8, and -S0T10, respectively. Recalled in Figure 5, there are around 45% of the crosslinked Ti—O—Ti polar segments dispersing on the surface of PIS-8%-S2T8. The strong crosslinkage between $Ti(OEt)_4$ groups or with $PhSiO(CH_3)_3$ produces polar Ti—O—Ti or Ti—O—Si chains on the surface. Some of the hydrophilic segments will be implanted on the film's surface leading to the decrease in contact angles. Notably, the contact angles of those Ti-containing hybrids are still larger than that of pure PI. The explanation is that more hydrophobic segments, —C_2H_6 and —CH_3, migrate to the surface of films due to the formation of strong crosslinkage by $Ti(OEt)_4$ groups.

Refractive Index and Birefringence

Optical devices, such as photonic integrated circuits and waveguide structures, generally require controlling the refractive index (RI, *n*). An increase in RI with the addition of $Ti(OEt)_4$ in polymer film has been observed, while the addition of PhSiOx provides a decrease in RI.[8] On the other hand, the benzene rings in PI will affect the penetration of polarized light from parallel or orthogonal direction into the film. Consequently, PI films possess specific birefringence characterization and optical compensate effect for c-plate LCD material usage.

Table III. Contact Angle and Dielectric Constant of Pure PI, PIS, and Hybrid Films

Sample	Contact angle (air-side) (°)	Dielectric constant
Pure PI	60.8	3.34
PIS	78.8	3.27
PIS-8%-S10T0	85.7	3.26
PIS-8%-S8T2	82.1	3.47
PIS-8%-S5T5	81.2	3.52
PIS-8%-S2T8	74.6	3.69
PIS-8%-S0T10	74.2	3.88

Table IV. Refractive Indices and Birefringence of Pure PI, PIS, and PI/PhSiOx/TiO_2 Hybrid Films

Sample	n_{TE}	n_{TM}	Δn
Pure PI	1.5937	1.6023	0.0085
PIS	1.5929	1.5962	0.0033
PIS-8%-S10T0	1.5923	1.5674	0.0249
PIS-8%-S8T2	1.5997	1.6284	0.0288
PIS-8%-S5T5	1.6052	1.6368	0.0316
PIS-8%-S2T8	1.6091	1.6506	0.0415
PIS-8%-S0T10	1.6040	1.6994	0.0954

n_{TE}: in-plane refractive index; n_{TM}: out-of-plane refractive index; and Δn: birefringence = $n_{TM} - n_{TE}$.

Table V. Color Intensity, Appearance, and Formability of Pure PI, PIS, and Hybrid Films

Sample	L^*	a^*	b^*	Appearance	Formability
Pure PI	86.1	−3.6	76.8	PY	F
PIS	87.5	−5.7	74.2	PY	F
PIS-8%-S10T0	87.1	−4.3	79.0	PY	F
PIS-8%-S8T2	76.4	9.3	67.7	Y	F
PIS-8%-S5T5	63.1	23.9	53.0	YB	F
PIS-8%-S2T8	46.6	30.8	27.0	YB	F
PIS-8%-S0T10	41.2	26.0	16.1	B	C

PY, pale yellow; B, brown; YB, yellow brown; Y, yellow; F, flexible; and C, crack.

Therefore, PI films may provide a broad application in optical fields.

As listed in Table IV, the difference between n_{TE} (ordinary light, parallel to the film)[31] values of samples is not significant. In contrast, the n_{TM} (extraordinary light, orthogonal to film)[31] values decrease from 1.6023 for pure PI to 1.5962 and 1.5674 for pure PIS and PIS-8%-S10T0, respectively. The addition of APrTMOS or PhSiOx induces loose PI matrix that the rays can easily pass through the film and the corresponding n_{TM} value is small. On the other hand, the n_{TM} values are increased from 1.5674 for PIS-8%-S10T0 to 1.6284, 1.6368, 1.6506, and 1.6994 for PIS-8%-S8T2, -S5T5, -S2T8, and -S0T10, respectively, with the corresponding titanium content of 0 to 1.6, 4.0, 6.4, and 8 wt % in hybrids. One of the reasons for the increase in n_{TM} is because the high RI of TiO_2 itself. The increase in n_{TM} values may also because the formation of dense and relatively stronger intermolecular crosslinkages from $Ti(OEt)_4$ groups.

Optical Transparency and Color Intensity

As displayed in Figure 11, the UV–vis spectra of pure PI and PIS films are similar. The optical transmission at 550 nm is around 83% for both pure PI and PIS films. The low optical transparency of PI derived from the practically cheap monomers BTDA and p-BAPP is expected.[32] The addition of 8% of PhSiOx in PI matrix slightly decreased the optical transparency. However, the optical transparency of PIS hybrid films decreased dramatically as the content of TiO_2 increased. For PIS-8%-S10T0 hybrid, the optical transmission at 550 nm is 82% compared to 15% for PIS-8%-S0T10 sample. The changes of optical transparency and color intensity with the composition of hybrid present the same trend of the above discussed properties.

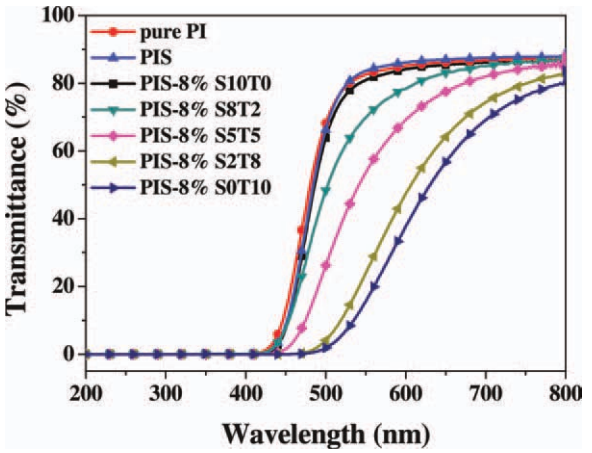

Figure 11. UV–vis spectra of pure PI and PIS hybrid films. [Color figure can be viewed in the online issue, which is available at wileyonlinelibrary.com.]

In this study, the lightness (L^*) index of PIS hybrid films is focused and listed in Table V together with yellowness (b^*) and redness (a^*) indices. A wide range of L^* values of all prepared films are presented ranging from 41.2 to 87.5. The apparent difference in L^* values of films is affected significantly by the Ti content but slightly by Si content. The L^* value is 86.1 for pure PI and slightly increases to 87.5 and 87.1 for pure PIS and PIS-8%-S10T0, respectively, due to the addition of APrTMOS or PhSiOx in the PI matrix. It is because that the loosely intermolecular crosslinkage is formed between the PhSi-$(OCH_3)_3$ groups and the free volume within polymer matrix is enlarged. On the other perspective, L^* values of hybrids with mixed PhSiOx and TiO_2 contents decrease from 87.1 for PIS-8%-S10T0 to 76.4, 63.1, 46.6, and 41.2 for PIS-8%-S8T2, -S5T5, -S2T8, and -S0T10, respectively. The active $Ti(OEt)_4$ groups are believed to induce the dense intermolecular crosslinkage and to decrease the free volume that the decrease in L^* value with Ti contents was observed.

CONCLUSIONS

Polyimide/PhSiOx-TiO_2 hybrid thin films for optical usages were prepared by using an *in situ* sol–gel process. The distributions of metal oxides within films are revealed by XPS analysis. The Si elements from APrTMOS and PhSiOx tend to migrate from the bulk to the surface of PI hybrids, while the Ti elements present a reverse trend. The presence of Si—O—Si, Ti—O—Ti, and Si—O—Ti bondings within the hybrids prove the crosslinked structures between PhSiOx and $Ti(OEt)_4$. The thermal decomposition temperature (Td) at 5% weight loss is in the range of 470 to 528°C. A higher T_g value of hybrids is presented than that of pure PI. The increase in TiO_2 content in hybrids increases the T_g values. The effects of TiO_2 on T_g values

and damping intensity are more significant than that of PhSiOx. The dielectric constants decrease upon the addition of PhSiOx due to the reduced free volume, while increase with titania content. The contact angles of PI hybrids increase with the increasing PhSiOx content, while the surface energies decrease, due to the dispersion of Si elements on the film's surface. The refractive index of PI/PhSiOx-TiO_2 hybrid is higher than that of other polymers and the hybrids show birefringence characteristics. The L^* values of PI/PhSiOx/TiO_2 hybrids, ranging from 41.2 to 87.5, are significantly affected by the Ti content. The best mixed oxide composition of the hybrid obtained in this study is 20/80, i.e., the compromised weight ratio of SiO_2/TiO_2, for inducing the superior properties for industrial applications.

REFERENCES

1. Cornelius, C. J.; Marand, E. *Polymer* **2002,** *43*, 2385.
2. Delozier, D. M.; Orwoll, R. A.; Cahoon, J. F.; Johnston, N. J.; Smith, J. G. *Polymer* **2002,** *43*, 813.
3. Cheong, S. I.; Choi, K. Y. *J. Appl. Polym. Sci.* **1995,** *55*, 1819.
4. Chen, Y.; Iroh, J. O. *Chem. Mater.* **1999,** *11*, 1218.
5. Tsai, M. H.; Lin, Y. K.; Chang, C. J.; Chiang, P. C.; Yeh, J. M.; Chiu, W. M.; Huang, S. L.; Ni, S. C. *Thin Solid Films* **2009,** *517*, 5333.
6. Hedrick, J. L.; Cha, H. J.; Miller, R. D.; Yoon, D. Y.; Brown, H. R.; Srinivasan, S.; Pietro, R.; Cook, R. F.; Hummel, J. P.; Klaus, D. P.; Liniger, E. G.; Simonyi, E. E. *Macromolecules* **1997,** *30*, 8512.
7. Tsai, M. H.; Whang, W. T. *Polymer* **2001,** *42*, 4197.
8. Tsai, M. H.; Liu, S. J.; Chiang, P. C. *Thin Solid Films* **2006,** *515*, 1126.
9. Duo, S.; Li, M.; Zhu, M.; Zhou, Y. *Mater. Chem. Phys.* **2008,** *112*, 1093.
10. Cheng, S.; Shen, D.; Zhu, X.; Tian, X.; Zhou, D.; Fan, L. J. *Eur. Polym. J.* **2009,** *45*, 2767.
11. Chavez, R.; Ionescu, Z.; Fasel, C.; Riedel, R. *Chem. Mater.* **2010,** *22*, 3823.
12. Kim, H. J.; Nam, S. M. *Ceram. Process. Res.* **2009,** *10*, 817.
13. Wang, S. F.; Wang, Y. R.; Cheng, K. C.; Chen, S. H. *J. Mater. Sci. Mater. Electron.* **2010,** *21*, 104.
14. Liaw, W. C.; Chen, K. P. *J. Appl. Polm. Sci.* **2007,** *105*, 809.
15. Liaw, W. C.; Chen, K. P. *Eur. Polym. J.* **2007,** *43*, 2265.
16. Liu, L.; Lu, Q. H.; Yin, J.; Zhu, Z. K.; Pan, D. C.; Wang, Z. G. *Mater. Sci. Eng. C* **2002,** *22*, 61.
17. Wang, H.; Zhong, W.; Xu, P.; Du, Q. *Composites A* **2005,** *36*, 909.
18. Liaw, W. C.; Cheng, Y. L.; Liao, Y. S.; Chen, C. S.; Lai, S. M. *Polym. J.* **2011,** *43*, 249.
19. Jung, S. M.; Dupont, O.; Grange, P. *Appl. Catal. A* **2001,** *208*, 393.
20. Almeida, R. M.; Vasconcelos, H. C.; Goncëalves, M. C.; Santos, L. F. *J. Non-Cryst. Solids* **1998,** *232-234*, 65.
21. Qiu, W.; Luo, Y.; Chen, F.; Duo, Y.; Tan H. *Polymer* **2003,** *44*, 5821.
22. Reddy, B. M.; Chowdhury, B.; Reddy, E. P.; Fernández, A. *Langmuir* **2001,** *17*, 1132.
23. Majumdar, A.; Das, G.; Patel, N.; Mishra, P.; Ghose, D.; Hippler, R. J. *Electrochem. Soc.* **2008,** *155*, D22.
24. Kannan, A. G.; Choudhury, N. R.; Dutta, N. K. *Polymer* **2007,** *48*, 7078.
25. Li, L.; Lu, Q. H.; Jie, Y.; Zikang, Z.; Daocheng, P.; Zongguang, W. *Mater. Sci. Eng. C* **2002,** *22*, 61.
26. Chiang, P. C.; Whang, W. T.; Wu, S. C.; Chuang, K. R. *Polymer* **2003,** *44*, 2249.
27. Jwo, S. L.; Whang, W. T.; Hsieh, T. E.; Pan, F. M.; Liaw, W. C. *J. Polym. Res* **1999,** *6*, 175.
28. Tsai, M. H.; Whang, W. T. *J. Appl. Polym. Sci.* **2001,** *81*, 2531.
29. Tsai, M. H.; Huang, S. L.; Chen, P. J.; Chiang, P. C.; Chen, D. S.; Lu, H. H.; Chiu, W. M.; Chen, J. C.; Lu, T. L. *Desalination* **2008,** *233*, 232.
30. Duo, S. W.; Li, M. S.; Zhu, M.; Zhou, Y. C. *Mater. Chem. Phys.* **2008,** *112*, 1093.
31. Terui, Y.; Ando, S. J. *Photopolym. Sci. Technol.* **2005,** *18*, 337.
32. Ando, S.; Matsuura, T.; Sasaki, S. *Polym. J.* **1997,** *29*, 69.